Advances in Nano Research, *Vol. 11, No. 6 (2021) 581-593*
https://doi.org/10.12989/anr.2021.11.6.581

A cylindrical shell model for nonlocal buckling behavior of CNTs embedded in an elastic foundation under the simultaneous effects of magnetic field, temperature change, and number of walls

Abdelaziz Timesli*

Hassan II University of Casablanca, National Higher School of Arts and Crafts (ENSAM CASABLANCA), AICSE Laboratory, 20670 Casablanca, Morocco

(*Received May 30, 2021, Revised August 15, 2021, Accepted August 17, 2021*)

Abstract. This model is proposed to describe the buckling behavior of Carbon Nanotubes (CNTs) embedded in an elastic medium taking into account the combined effects of the magnetic field, the temperature, the nonlocal parameter, the number of walls. Using Eringen's nonlocal elasticity theory, thin cylindrical shell theory and Van der Waal force (VdW) interactions, we develop a system of partial differential equations governing the buckling response of CNTs embedded on Winkler, Pasternak, and Kerr foundations in a thermal-magnetic environment. The pre-buckling stresses are obtained by applying airy's stress function and an adjacent equilibrium criterion. To estimate the nonlocal critical buckling load of CNTs under the simultaneous effects of the magnetic field, the temperature change, and the number of walls, an optimization technique is proposed. Furthermore, analytical formulas are developed to obtain the buckling behavior of SWCNTs embedded in an elastic medium without taking into account the effects of the nonlocal parameter. These formulas take into account VdW interactions between adjacent tubes and the effect of terms involving differences in tube radii generally neglected in the derived expressions of the critical buckling load published in the literature. Most scientific research on modeling the effects of magnetic fields is based on beam theories, this motivation pushes me to develop a cylindrical shell model for studying the effect of the magnetic field on the static behavior of CNTs. The results show that the magnetic field has significant effects on the static behavior of CNTs and can lead to slow buckling. On the other hand, thermal effects reduce the critical buckling load. The findings in this work can help us design of CNTs for various applications (e.g. structural, electrical, mechanical and biological applications) in a thermal and magnetic environment.

Keywords: buckling behavior of CNTs; cylindrical shell theory; elastic foundations; Multi Walled Carbon Nanotubes (MWCNTs); nonlocal elasticity theory; small-scale effects; thermal and magnetic environment; Van der Waals (VdW) interaction

1. Introduction

Iijima (1991) of the NEC Laboratory (Tsukuba, Japan) discovered of carbon nanotubes (CNTs) in 1991. Since this time, there was a lot of research work on CNTs. For the study of the mechanical behavior of CNTs, we find in the literature atomistic-based methods (Yacobson *et al*. 1996, Hernandez *et al*. 1998, Sanchez-Portal *et al*. 1996). Using these methods in molecular dynamics (MD) simulation of buckling behavior, Liew at al. (2004) explain that the calculation for a SWCNTs (10,10) with 2000 atoms required 36 hours on a single CPU SGI origin 2000 system, which shows that these methods are very expensive in terms of computing time and thus this time explodes exponentially with MWCNTs. Also, the experiment measurements are often complex at the nanoscale level for the investigations of the mechanical behaviors of SWCNTs, DWCNTs and MWCNTs (see Fig. 1). Wherefore, several authors propose to analyze of SWCNTs and MWCNTs using continuum mechanics methods, such as (Jena *et al*. 2020, Yazid *et al*. 2018, Wu *et al*. 2018, Karami *et al* 2018, Timesli 2020, Iijima *et al*. 1996, Falvo *et al*. 1997, Mohamed *et al*. 2020, Malikan 2020, Rahmani and Antonov 2019, Xie *et al*. 2020, Asghar *et al*. 2020, Hussain *et al*. 2020). In continuum theories, Eringen's nonlocal elasticity theory has been successfully used to analyze the static deflection, bending, buckling, wave propagation, vibration and instability analysis of CNTs (Eringen 1972a, b, 1983, 2002, Eringen and Edelen 1972). Note that the small-scale effect for micro- and nanostructures is very important and we can take it into account by the Eringen's nonlocal elasticity theory. Although, some works in literature have used the nonlocal continuum mechanics to present theoretical investigations of the CNTs (Matouk *et al*. 2020, Asghar *et al*. 2020, Taj *et al*. 2020, Balubaid *et al*. 2020, Hussain *et al*. 2019, Boutaleb *et al*. 2019, Berghouti *et al*. 2019). Other authors are interested to study of SWCNTs and MWCNTs embedded in a polymer or a metal matrix, such as (Bensattalah *et al*. 2018, Calvert 1999, Gul and Aydogdu 2018, Jena *et al*. 2020, Kuzumaki *et al* 1998, Karami *et al*. 2018, Malikan and Eremeyev 2020, Schadler *et al*. 2018, Wu *et al*. 2018, Zhou *et al*. 2019). The excellent properties and high strength to weight ratio of the CNTs

*Corresponding author, Ph.D., Professor
E-mail: ABDELAZIZ.TIMESLI@univh2c.ma;
abdelaziz.timesli@gmail.com

ISSN: 2287-237X (Print), 2287-2388 (Online)

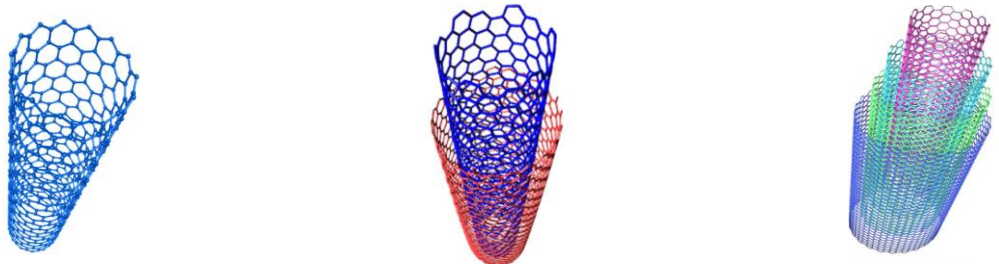

(a) SWCNTs (b) DWCNTs (c) MWCNTs

Fig. 1 Schematic for simply-supported CNTs

have greatly aided to develop nanostructures which are used in nanomechanical, nanoelectronics, nanobiological, nano-devices, and nanocomposites systems. Nanostructures are mainly used as reinforcing material as indicated in the literature (Zerrouki *et al*. 2021, Heidari *et al*. 2021, Bendenia *et al*. 2020, Al-Furjan *et al*. 2020a, b, c, d, Bourada *et al*. 2020, Bousahla *et al*. 2020, Al-Furjan *et al*. 2021, Timesli 2020a). Furthermore, the existence of porosities can affect considerably of nanostructures for a more efficient manufacturing of these types of materials and their technical design (Medani *et al*. 2019, Arshid *et al*. 2021, Timesli 2021). There are also other kinds of applications of nanostructure as shown in recent years by researchers to provide a perfect understanding of the properties of these materials. As examples, Van Vinh and Tounsi (2021) studied the effect of the spatial variation of the nonlocal parameter on the Functionally Graded (FG) sandwich nanoplates. Soleimani-Javid *et al*. (2021) examined the vibrational behavior of a sandwich plate consisting of flexoelectric face sheets and honeycomb core. The study of the buckling behavior of a graphene sheet embedded in a visco-Pasternak medium is investigated by Bellal *et al*. (2020) and Rouabhia *et al*. (2020). Karami *et al*. (2019b) studied the buckling behavior of FG nanoplates made of anisotropic material. Rai and Bajpai (2021) discussed recent developments in the treatment of ZnO nanostructures, their characterizations by various techniques and their future perspective. Wang *et al*. (2021) studied the buckling behavior of two-dimensional FG nanotubes, including porosity using first shear deformation and higher-order theory. Ebrahimi *et al*. (2020) presented a comprehensive review on the piezoelectric behavior of nanostructures, they are interested in understanding the properties of piezoelectric structures intended for use in electromechanical systems.

In a variety of applications (ultra-high-density magnetic recording media, magnetic resonance imaging, sensing, hyperthermia, catalysts … etc), magnetic nanostructures are considered as a novel class of materials. According to growing conditions, various forms (nanoparticles, nano-wires, nanotubes, multilayers … etc) can be used to synthesize these types of nanostructures. The magnetic field effect on nanostructures has been investigated by researchers (Sobamowo *et al*. 2021, Ponnusamy and Amuthalakshmi 2015, Cao *et al*. 2020, Arda and Aydogdu 2018, Ajiki and Ando 1996, Fedorov *et al*. 2007, Bellucci *et al*. 2007, Lee *et al*. 2018, Karami *et al*. 2019a). Ajiki and Ando (1996) investigated the electronic states of CNTs in a magnetic field. Bellucci *et al*. (2007) studied the transport properties of CNTs under the effect of the vertical magnetic field. Ponnusamy and Amuthalakshmi (2015) investigated the transverse vibration of DWCNTs under thermal and magnetic fields, the model used in this study is based on nonlocal Timoshenko beam theory. Recently, Lee *et al*. (2018) modeled magnetically driven torsional actuation of a MWCNT yarn artificial muscle. Karami *et al*. (2019a) studied the wave dispersion response of nanoshell made of FG anisotropic material, they evaluated the influences of several parameters including the magnetic field intensity. Sobamowo *et al*. (2021) used Euler-Bernoulli beam theories coupled with Eringen's nonlocal elasticity and VdW forces equation to investigate the nonlinear transverse vibrations of CNTs embedded on elastic foundations. This study took into account the combined effects of several parameters, such as magnetic field, small scales, temperature, and number of layers. Cao *et al*. (2020) presented recent advances of magnetic fields effects on the manipulation of nanostructures.

Most research has focused on studying the effects of internal and external parameters on nanostructures. Also in scientific research, beam theories are most used to study the effects of magnetic fields. Motivated by these works in the literature, we develop a cylindrical continuum shell model to study the simultaneous effects of the magnetic field, the temperature change, the number of walls, and the nonlocal parameter of CNTs embedded in Winkler, Pasternak, and Kerr elastic foundations. The equivalent values of the Young modulus and the shell thickness are required to use of the continuum model of CNT structure, they can be determined by the molecular dynamic simulation and the continuum mechanics shell models. For modeling of CNTs, we propose to use the continuum model based on the theory of circular cylindrical shells and the simplifying shallow-shell hypothesis, which is developed by Donnell (1934). We chose this theory for the reason that it is relatively simple and practically accurate considering the following hypotheses: (lengh/radius) $\geq$ 10, (thickness/radius)$^2 \ll 1$, $(1/\text{circumferential half wavenumber})^2 \ll 1$. To simplify the problem (the three equations of equilibrium involving the shell displacements in the radial, circumferential and axial directions) we reduce the number of equations to two involving only the radial displacement and the stress function. Using Eringen's nonlocal elasticity, Donnell shell (Donnell 1934, Timesli 2020a, b, c) theories and VdW forces interaction, the buckling responses of CNTs embedded on Winkler, Pasternak, and Kerr foundations in a

thermal and magnetic environment are developed. We develop analytical solutions for local buckling and we present parametric studies with discussion of results. Note that in this study my previous work (Timesli 2020b) on DWCNTs embedded in an elastic foundation is generalized for MWCNT and SWCNT with applied magnetic field effect under thermal environment and taking into account the effects of internal small length scale and VdW interactions. One of the novelties of the present work with respect to the open literature for studying the effects of magnetic fields on CNTs is the use of cylindrical shell model and Kerr foundation.

2. Model development based on the nonlocal cylindrical shell theory for SWCNTs and MWCNTs resting on elastic foundations

Consider a SWCNT subjected to an external axial pressure and resting on elastic foundations under the influences of temperature and magnetic field as shown in Fig. 2.

Using our previous studies (Timesli 2020a, b, c) and taking into account the combined effects of the magnetic field, temperature and nonlocal parameter, we can find the development of the governing equation of the motion for the embedded CNTs on elastic foundation. Using the Eringen's nonlocal elasticity theory, Donnell shell theory and Hamilton's principle, the equilibrium equation for the SWCNT is given as follows:

$$\begin{aligned} &D\Delta^2 w-(1-(e_0a)^2\nabla^2)\\ &\left(\frac{N_{\theta\theta}}{R}+\left(N_{xx}+\frac{Eh\alpha_x}{1-\upsilon}\Delta T+\eta hH_x^2\right)\frac{\partial^2 w}{\partial x^2}\right.\\ &\left.+2\frac{N_{x\theta}}{R}\frac{\partial^2 w}{\partial x\partial\theta}+\frac{N_{\theta\theta}}{R^2}\frac{\partial^2 w}{\partial\theta^2}-f\right)=0 \end{aligned} \tag{1}$$

where $\Delta^2=\left(\frac{\partial^2}{\partial x^2}+\frac{1}{R^2}\frac{\partial^2}{\partial\theta^2}\right)^2$ and f can be written by the following relation (Timesli 2017, 2020a, b, c):

$$f=\frac{1}{1+\chi\frac{K_W}{K_K}}\left(K_W w-K_P\nabla^2 w-\frac{DK_P}{K_K}\nabla^6 w\right) \tag{2}$$

with $\chi=K_P=K_K=0$ for Winkler foundation, $\chi=K_K=0$ for Pasternak foundation and $\chi=1$ for Kerr foundation.

To study the thermal field effect, we consider the values of the coefficient of thermal expansion measured by Deng *et al*. (2014) using Raman spectroscopy. They showed that $\alpha_x=(-1.9\pm0.6)\times10^{-5}\mathrm{K}^{-1}$ for SWCNTs and $\alpha_x=(-2.1\pm0.7)\times10^{-5}\mathrm{K}^{-1}$ for DWCNTs at room temperature. The thermal behavior of CNTs is significantly disturbed by the existence of a surrounding environment (Yan *et al*. 2012). The presence of strong interactions between CNTs and substrates gives a coefficient of thermal expansion bigger than $2.0\times10^{-5}\mathrm{K}^{-1}$ as shown by Jiang *et al*. (2009). Due to simplification we choose the value $\alpha_x=2.5\times10^{-5}\mathrm{K}^{-1}$ in the present study.

Note that the membrane forces can be connected to the stress function ϕ as follows:

$$N_{xx}=\frac{Eh}{R^2}\frac{\partial^2\phi}{\partial\theta^2},\qquad N_{\theta\theta}=Eh\frac{\partial^2\phi}{\partial x^2},\qquad N_{x\theta}=\frac{Eh}{R}\frac{\partial^2\phi}{\partial x\partial\theta} \tag{3}$$

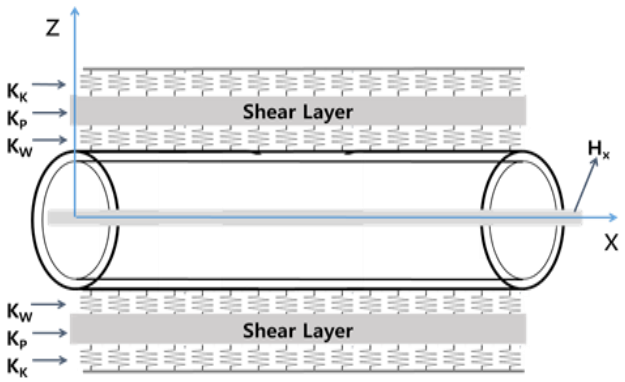

Fig. 2 Schematic for simply supported embedded SWCNT on three-parameter elastic foundation

We can study the possible existence of adjacent equilibrium configurations using the adjacent equilibrium criterion (Brush and Almroth 1975). We assume that the indices 0 and b indicate, respectively, pre-buckling and post-buckling quantities and we neglect the terms of second order in index b to demonstrate that:

$$\begin{aligned} &k\Delta^2 w_b-(1-(e_0a)^2\nabla^2)\\ &\frac{1}{Eh}\left(\frac{Eh}{R}\frac{\partial^2\phi}{\partial x^2}+\left(N_{xx0}+\frac{Eh\alpha_x}{1-\upsilon}\Delta T+\eta hH_x^2\right)\frac{\partial^2 w_b}{\partial x^2}\right.\\ &+2\frac{N_{x\theta0}}{R}\frac{\partial^2 w_b}{\partial x\partial\theta}+\frac{N_{\theta\theta0}}{R^2}\frac{\partial^2 w_b}{\partial\theta^2}\\ &\left.-\frac{1/(Eh)}{\left(1+\chi\frac{K_W}{K_K}\right)}\left(K_W w_b-K_P\nabla^2 w_b-\frac{DK_P}{K_K}\nabla^6 w_b\right)\right)=0 \end{aligned} \tag{4}$$

The stress function $\phi(x,\theta)$ verifies the compatibility condition (Timesli 2020b, c), which gives the following equation:

$$\Delta^2\phi+\rho\frac{\partial^2 w_b}{\partial x^2}-(e_0a)^2\begin{pmatrix}\frac{\partial^6\phi}{\partial x^6}+3\rho^2\frac{\partial^6\phi}{\partial x^4\partial\theta^2}\\+3\rho^4\frac{\partial^6\phi}{\partial x^2\partial\theta^4}+\rho^6\frac{\partial^6\phi}{\partial\theta^6}\end{pmatrix}=0 \tag{5}$$

where $\rho=1/R$.

Neglecting the shear membrane forces ($N_{x\theta0}=0$) and the circumferential membrane force ($N_{\theta\theta0}=0$), the system (4)-(5) becomes:

$$\begin{cases} k^2\Delta^2 w_b-(1-(e_0a)^2\nabla^2)\\ \quad\left(\rho\frac{\partial^2\phi}{\partial x^2}+\frac{1}{Eh}\left(U+\frac{Eh\alpha_x}{1-\upsilon}\Delta T+\eta hH_x^2\right)\frac{\partial^2 w_b}{\partial x^2}\right.\\ -\frac{1/(Eh)}{\left(1+\chi\frac{K_W}{K_K}\right)}\left(K_W w_b-K_P\nabla^2 w_b-\frac{DK_P}{K_K}\nabla^6 w_b\right)\Big)=0\\ \Delta^2\phi+\rho\frac{\partial^2 w_b}{\partial x^2}\\ \quad-(e_0a)^2\begin{pmatrix}\frac{\partial^6\phi}{\partial x^6}+3\rho^2\frac{\partial^6\phi}{\partial x^4\partial\theta^2}\\+3\rho^4\frac{\partial^6\phi}{\partial x^2\partial\theta^4}+\rho^6\frac{\partial^6\phi}{\partial\theta^6}\end{pmatrix}=0 \end{cases} \tag{6}$$

where U is the axial compression ($U=N_{xx0}$).

Consider N layers which is represented by $i$with $i=1,2,3,\ldots,N$. The interaction between MWCNTs and the elastic foundation takes place through the outer tube. So in

the governing equation, we include the elastic foundation terms only for the outer tube. The development of the expression for VdW force between two successive tubes is based on the fact the pressure at any point between any two adjacent tubes depends on the difference of their deflections at that point (Ru 2000, Aminikhah and Hemmatnezhad 2011, Fu *et al*. 2006, Yacobson *et al*. 1996, Liew *et al*. 2004) as follows:

$$\begin{cases} F_i = c_i\,(w_{i+1} - w_i) \\ c_i = -\left[\dfrac{1001\pi\xi\sigma^{12}}{3a^4}E_i^{13} - \dfrac{1120\pi\xi\sigma^{6}}{9a^4}E_i^{7}\right]R_{i+1} \\ E_i^m = \dfrac{1}{(R_i + R_{i+1})^m}\displaystyle\int_0^{\frac{\pi}{2}} \frac{d\theta}{(1 - K_i\,cos^2(\theta))^{m/2}}R_{i+1} \\ K_i = \dfrac{4R_iR_{i+1}}{(R_i + R_{i+1})^2} \end{cases} \tag{7}$$

with $\xi = 2.968meV$ and $\sigma = 0.3407nm$.

Consequently, using the pressure of elastic foundation and the VdW forces, the developed equilibrium equations of the embedded MWCNT in a thermal and magnetic environment with N layers are given as:

$$\begin{cases} k^2\Delta_1^2 w_1 - (1 - (e_0a)^2\nabla_1^2) \\ \left(\dfrac{1}{Eh}\left(U + \dfrac{Eh\alpha_x}{1-\upsilon}\Delta T + \eta h H_x^2\right)\dfrac{\partial^2 w_1}{\partial x^2}\right. \\ \left. +\rho_1\dfrac{\partial^2\phi_1}{\partial x^2} - \dfrac{c_1}{Eh}\,(w_2 - w_1)\right) = 0 \\ \Delta_1^2\phi_1 + \rho_1\dfrac{\partial^2 w_1}{\partial x^2} \\ -(e_0a)^2\begin{pmatrix} \dfrac{\partial^6\phi_1}{\partial x^6} + 3\rho_1^2\dfrac{\partial^6\phi_1}{\partial x^4\partial\theta^2} \\ +3\rho_1^4\dfrac{\partial^6\phi_1}{\partial x^2\partial\theta^4} + \rho_1^6\dfrac{\partial^6\phi_1}{\partial\theta^6} \end{pmatrix} = 0 \end{cases} \tag{8}$$

$$\begin{cases} k^2\Delta_2^2 w_2 - (1 - (e_0a)^2\nabla_2^2) \\ \left(\dfrac{1}{Eh}\left(U + \dfrac{Eh\alpha_x}{1-\upsilon}\Delta T + \eta h H_x^2\right)\dfrac{\partial^2 w_2}{\partial x^2}\right. \\ \left. +\rho_2\dfrac{\partial^2\phi_2}{\partial x^2} - \dfrac{c_2}{Eh}(w_3 - w_2) + \dfrac{c_1}{Eh}(w_2 - w_1)\right) = 0 \\ \Delta_2^2\phi_2 + \rho_2\dfrac{\partial^2 w_2}{\partial x^2} \\ -(e_0a)^2\begin{pmatrix} \dfrac{\partial^6\phi_2}{\partial x^6} + 3\rho_2^2\dfrac{\partial^6\phi_2}{\partial x^4\partial\theta^2} \\ +3\rho_2^4\dfrac{\partial^6\phi_2}{\partial x^2\partial\theta^4} + \rho_2^6\dfrac{\partial^6\phi_2}{\partial\theta^6} \end{pmatrix} = 0 \end{cases} \tag{9}$$

$$\begin{cases} k^2\Delta_3^2 w_3 - (1 - (e_0a)^2\nabla_3^2) \\ \left(\dfrac{1}{Eh}\left(U + \dfrac{Eh\alpha_x}{1-\upsilon}\Delta T + \eta h H_x^2\right)\dfrac{\partial^2 w_3}{\partial x^2}\right. \\ \left. +\rho_3\dfrac{\partial^2\phi_3}{\partial x^2} - \dfrac{c_3}{Eh}(w_4 - w_3) + \dfrac{c_2}{Eh}(w_3 - w_2)\right) = 0 \\ \Delta_3^2\phi_3 + \rho_3\dfrac{\partial^2 w_3}{\partial x^2} \\ -(e_0a)^2\begin{pmatrix} \dfrac{\partial^6\phi_3}{\partial x^6} + 3\rho_3^2\dfrac{\partial^6\phi_3}{\partial x^4\partial\theta^2} \\ +3\rho_3^4\dfrac{\partial^6\phi_3}{\partial x^2\partial\theta^4} + \rho_3^6\dfrac{\partial^6\phi_3}{\partial\theta^6} \end{pmatrix} = 0 \end{cases} \tag{10}$$

$$\begin{cases} k^2\Delta_N^2 w_N - (1 - (e_0a)^2\nabla_N^2) \\ \left(\dfrac{1}{Eh}\left(U + \dfrac{Eh\alpha_x}{1-\upsilon}\Delta T + \eta h H_x^2\right)\dfrac{\partial^2 w_N}{\partial x^2}\right. \\ \left. +\rho_N\dfrac{\partial^2\phi_N}{\partial x^2} + \dfrac{c_{N-1}}{Eh}(w_N - w_{N-1})\right) \\ -\dfrac{1/(Eh)}{\left(1 + \chi\frac{K_W}{K_K}\right)}\left(K_W w_N - K_P\nabla^2 w_N - \dfrac{DK_P}{K_K}\nabla^6 w_N\right)\Big) = 0 \\ \Delta_N^2\phi_N + \rho_N\dfrac{\partial^2 w_N}{\partial x^2} \\ -(e_0a)^2\begin{pmatrix} \dfrac{\partial^6\phi_N}{\partial x^6} + 3\rho_N^2\dfrac{\partial^6\phi_N}{\partial x^4\partial\theta^2} \\ +3\rho_N^4\dfrac{\partial^6\phi_N}{\partial x^2\partial\theta^4} + \rho_3^6\dfrac{\partial^6\phi_N}{\partial\theta^6} \end{pmatrix} = 0 \end{cases} \tag{11}$$

3. Solution methodology for buckling analysis of embedded MWCNTs on elastic foundation under coupled effects of magnetic field and temperature change

The solution of the problem for embedded MWCNTs on elastic foundation under coupled effects of magnetic field and temperature change is sought in the following form (Timesli *et al*. 2017, 2020b):

$$\begin{cases} w_j(x,\theta) = A_j\,exp\left(i\dfrac{m\pi}{L}x\right)cos(n\theta) \\ \phi_j(x,\theta) = a_j\,exp\left(i\dfrac{m\pi}{L}x\right)cos(n\theta) \end{cases} \tag{12}$$

where A_j and a_j are arbitrary complex constants, n and m are respectively the circumferential and axial half wavenumbers of the jth tube. Substituting of the solution (12) in the system of Eqs. (8)-(11) and we obtain:

$j = 1$:

$$\begin{cases} [\alpha_1 - \lambda\eta_1 p^2]A_1 + \dfrac{\gamma_1 c_1}{E\hbar}A_2 = 0 \\ \alpha_1 = k^2(1 + \beta_1^2)^2 p^4 - \dfrac{\gamma_1}{E\hbar}\left(\dfrac{E\hbar\alpha_x}{1-\upsilon}\Delta T + \eta\hbar H_x^2\right)p^2 \\ \quad + \dfrac{\rho_1^2\gamma_1}{(1 + \beta_1^2)^2 + \mu^2(1 + 3\beta_1^2 + 3\beta_1^4 + \beta_1^6)p^2} - \dfrac{\gamma_1 c_1}{E\hbar} \end{cases} \tag{13}$$

$2 \le j \le N - 1$:

$$\begin{cases} \left[\alpha_j - \lambda\eta_j p^2\right]A_j + \dfrac{\gamma_j c_j}{E\hbar}A_{j+1} + \dfrac{\gamma_{j-1}c_{j-1}}{E\hbar}A_{j-1} = 0 \\ \alpha_j = k^2\left(1 + \beta_j^2\right)^2 p^4 - \dfrac{\gamma_1}{E\hbar}\left(\dfrac{E\hbar\alpha_x}{1-\upsilon}\Delta T + \eta\hbar H_x^2\right)p^2 \\ \quad + \dfrac{\rho_j^2\gamma_j}{\left(1 + \beta_j^2\right)^2 + \mu^2\left(1 + 3\beta_j^2 + 3\beta_j^4 + \beta_j^6\right)p^2} \\ \quad - \dfrac{\gamma_j\left(c_j + c_{j-1}\right)}{E\hbar} \end{cases} \tag{14}$$

$j = N$:

$$\begin{cases} [\alpha_N - \lambda\gamma_N p^2]A_N + \dfrac{\gamma_{N-1}c_{N-1}}{E\hbar}A_{N-1} = 0 \\ \alpha_N = k^2(1+\beta_N^2)^2p^4 - \dfrac{\gamma_N}{E\hbar}\left(\dfrac{E\hbar\alpha_x}{1-\upsilon}\Delta T + \eta\hbar H_x^2\right)p^2 \\ \quad + \dfrac{\rho_N^2\gamma_N}{(1+\beta_N^2)^2 + \mu^2(1+3\beta_N^2+3\beta_N^4+\beta_N^6)p^2} - \dfrac{\gamma_N c_{N-1}}{E\hbar} \\ \quad + \dfrac{1}{E\hbar}\left(1+\chi\dfrac{K_W}{K_K}\right)^{-1}[K_W + (K_P+\mu^2K_W)(1+\beta_N^2)p^2 \\ \quad + \mu^2K_P(1+2\beta_N^2+\beta_N^4)p^4 + \mathrm{D}\dfrac{K_P}{K_K}(1+3\beta_N^2+3\beta_N^4+\beta_N^6)p^6 \\ \quad + \mu^2 D\dfrac{K_P}{K_K}(1+4\beta^2+6\beta_N^4+4\beta_N^6+\beta_N^8)p^8] \end{cases} \quad (15)$$

where $p = m/L$, $q_j = n/R_j$, aspect ratios $\beta_j = \dfrac{q_j}{p}$ with $\beta_j = \left(\dfrac{R_{j-1}}{R_j}\right)\beta_{j-1}$ and $\gamma_j = \left(1+\mu^2\left(1+\beta_j^2\right)p^2\right)$.

Taking into account the system (13)-(15), we obtain the following homogeneous matrix system:

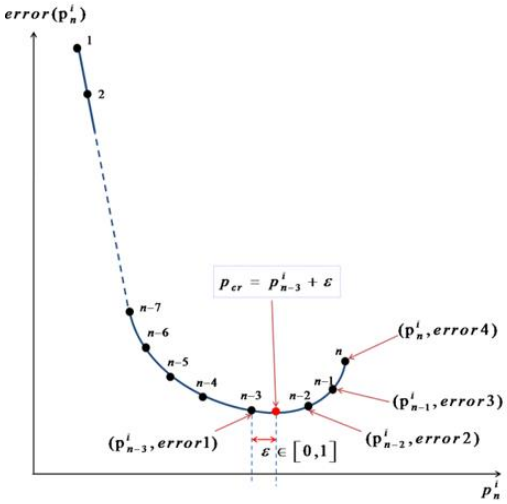

Fig. 3 Principle of finding the critical axial wave number p_{cr}

$$\begin{bmatrix} \alpha_1 - \lambda\gamma_1 p^2 & \dfrac{\gamma_1 c_1}{E\hbar} & 0 & 0 & \cdots & 0 & 0 \\ \dfrac{\gamma_1 c_1}{E\hbar} & \alpha_2 - \lambda\gamma_2 p^2 & \dfrac{\gamma_2 c_2}{E\hbar} & 0 & \cdots & 0 & 0 \\ 0 & \dfrac{\gamma_2 c_2}{E\hbar} & \alpha_3 - \lambda\gamma_3 p^2 & \dfrac{\gamma_3 c_3}{E\hbar} & \cdots & 0 & 0 \\ 0 & 0 & \dfrac{\gamma_3 c_3}{E\hbar} & \alpha_4 - \lambda\gamma_4 p^2 & \cdots & 0 & 0 \\ 0 & 0 & 0 & \dfrac{\gamma_4 c_4}{E\hbar} & \ddots & 0 & 0 \\ 0 & 0 & 0 & 0 & \cdots & \alpha_N - \lambda\gamma_N p^2 & \dfrac{\gamma_{N-1}c_{N-1}}{E\hbar} \\ 0 & 0 & 0 & 0 & 0 & \dfrac{\gamma_{N-1}c_{N-1}}{E\hbar} & \alpha_N - \lambda\gamma_N p^2 \end{bmatrix} \times \begin{Bmatrix} A_1 \\ A_2 \\ A_3 \\ A_4 \\ \vdots \\ A_{N-1} \\ A_N \end{Bmatrix} = [C(p,\beta_1,\beta_2,\ldots,\beta_N)] \begin{Bmatrix} A_1 \\ A_2 \\ A_3 \\ A_4 \\ \vdots \\ A_{N-1} \\ A_N \end{Bmatrix} = \begin{Bmatrix} 0 \\ 0 \\ 0 \\ 0 \\ \vdots \\ 0 \\ 0 \end{Bmatrix} \quad (16)$$

The system (16) of N equations and N unknowns $(A_1, A_2, A_3, \ldots, A_N)$ has a nonzero solution if its determinant is zero:

$$det([C(p,\lambda,\beta_1,\beta_2,\ldots,\beta_N)]) = 0 \quad (17)$$

The resolution of the expression of the determinant Eq. (17) gives the buckling loads λ for fixed values of aspect ratios β_1, β_2,... and β_N.The critical buckling load λ_{cr} is the smallest value of λ, this value is equivalent to the critical axial wave number p_{cr}. The resolution of the expression of the determinant Eq. (17) gives the buckling loads λ for fixed values of aspect ratios β_1, β_2,... and β_N. The critical buckling load λ_{cr} is the smallest value of λ, this value is equivalent to the critical axial wave number p_{cr}. The classical method for finding these critical values is the numerical minimization of the buckling load with respect to the axial wave number p.

In this research paper, we use the proposed algorithm as shown in Fig. 3 which allows us to determine quickly and automatically the best value of the critical axial wave number p_{cr}. So we can obtain the critical buckling load $\lambda_{cr} = \lambda(p_{cr})$. For a detail on this optimization technique, we refer the reader to the papers (Timesli 2020b, c).

4. Analytical solution based on the cylindrical shell theory for local buckling of embedded SWCNTs on elastic foundation under coupled effects of magnetic field and temperature change

In particular cases, we can develop analytical solutions based on the local elasticity theory for buckling of SWCNTs and DWCNTs. For SWCNTs embedded in an elastic medium under axial compression, the nonlocal critical buckling load is simplified as follows:

$$\lambda(p,\beta)=\frac{1}{\gamma p^2}\Bigg(\begin{matrix}k^2\left(1+\beta^2\right)^2p^4\\-\frac{\gamma}{E\hbar}\left(\frac{E\hbar\alpha_x}{1-\upsilon}\Delta T+\eta\hbar H_x^2\right)p^2\end{matrix}+\frac{\rho^2\gamma}{\left(1+\beta^2\right)^2+\mu^2\left(1+3\beta^2+3\beta^4+\beta^6\right)p^2}+\frac{1}{E\hbar}\left(1+\chi\frac{K_W}{K_K}\right)^{-1}\Big[K_W+\left(K_P+\mu^2K_W\right)\left(1+\beta^2\right)p^2+\mu^2K_P\left(1+2\beta^2+\beta^4\right)p^4+\mathrm{D}\frac{K_P}{K_K}\left(1+3\beta^2+3\beta^4+\beta^6\right)p^6+\mu^2D\frac{K_P}{K_K}\left(1+4\beta^2+6\beta^4+4\beta^6+\beta^8\right)p^8\Big]\Bigg) \tag{18}$$

In the case of local theory of elasticity, the nonlocal parameter $e_0=0$, which allows us to write:

$$\lambda(p,\beta)=k^2\left(1+\beta^2\right)^2p^2-\frac{1}{E\hbar}\left(\frac{E\hbar\alpha_x}{1-\upsilon}\Delta T+\eta\hbar H_x^2\right)+\frac{\rho^2}{\left(1+\beta^2\right)^2}+\frac{1}{E\hbar}\left(1+\chi\frac{K_W}{K_K}\right)^{-1}\left[\begin{matrix}\frac{K_W}{p^2}+K_P\left(1+\beta^2\right)\\+\mathrm{D}\frac{K_P}{K_K}\left(1+3\beta^2+3\beta^4+\beta^6\right)p^4\end{matrix}\right] \tag{19}$$

For fixed aspect ratio β, we can obtain the critical buckling load λ_{cr} by minimizing the buckling load $\lambda(p,\beta)$ in the Eq. (19) with respect to the axial wave number p:

$$\left.\frac{\partial\lambda(p,\beta)}{\partial p}\right|_{\beta\text{ fixed}}=0 \tag{20}$$

The Eq. (20) leads to a polynomial of degree 6 in p and by putting $\theta=p^2$ we can reduce the degree of the polynomial to 3:

$$\left(\frac{2\mathrm{D}}{E\hbar}\frac{K_P}{K_K}\left(1+\chi\frac{K_W}{K_K}\right)^{-1}\left(1+3\beta^2+3\beta^4+\beta^6\right)\right)\theta^3+\left(k^2\left(1+\beta^2\right)^2\right)\theta^2+\left(\frac{\rho^2}{\left(1+\beta^2\right)^2}-\frac{K_W}{E\hbar}\left(1+\chi\frac{K_W}{K_K}\right)^{-1}\right)=0 \tag{21}$$

Then we put $\varphi=\theta+\frac{k^2\left(1+\beta^2\right)^2}{3\left(\frac{2\mathrm{D}K_P}{E\hbar K_K}\left(1+\chi\frac{K_W}{K_K}\right)^{-1}\left(1+3\beta^2+3\beta^4+\beta^6\right)\right)}$ to rewrite Eq. (21) in the following form:

$$\varphi^3-\frac{1}{3}\left(\frac{k^2\left(1+\beta^2\right)^2}{\frac{2\mathrm{D}}{E\hbar}\frac{K_P}{K_K}\left(1+\chi\frac{K_W}{K_K}\right)^{-1}\left(1+3\beta^2+3\beta^4+\beta^6\right)}\right)^2\varphi+\frac{2}{27}\left(\frac{k^2\left(1+\beta^2\right)^2}{\frac{2\mathrm{D}}{E\hbar}\frac{K_P}{K_K}\left(1+\chi\frac{K_W}{K_K}\right)^{-1}\left(1+3\beta^2+3\beta^4+\beta^6\right)}\right)^3=0 \tag{22}$$

For the Eq. (22), we can demonstrate the flowing only real root:

$$\varphi=\sqrt[3]{-\frac{G_0}{2}+\sqrt{\frac{G_0^2}{4}+\frac{G_1^3}{27}}}+\sqrt[3]{-\frac{G_0}{2}-\sqrt{\frac{G_0^2}{4}+\frac{G_1^3}{27}}} \tag{23}$$

where

$$\begin{cases}G_1=-\frac{1}{3}\left(\frac{k^2\left(1+\beta^2\right)^2}{\frac{2\mathrm{D}}{E\hbar}\frac{K_P}{K_K}\left(1+\chi\frac{K_W}{K_K}\right)^{-1}\left(1+3\beta^2+3\beta^4+\beta^6\right)}\right)^2\\G_0=\frac{2}{27}\left(\frac{k^2\left(1+\beta^2\right)^2}{\frac{2\mathrm{D}}{E\hbar}\frac{K_P}{K_K}\left(1+\chi\frac{K_W}{K_K}\right)^{-1}\left(1+3\beta^2+3\beta^4+\beta^6\right)}\right)^3\end{cases} \tag{24}$$

So we can define p_{cr} as follows:

$$p_{cr}=\left(\varphi-\frac{k^2\left(1+\beta^2\right)^2}{3\left(\frac{2\mathrm{D}}{E\hbar}\frac{K_P}{K_K}\left(1+\chi\frac{K_W}{K_K}\right)^{-1}\left(1+3\beta^2+3\beta^4+\beta^6\right)\right)}\right)^{\frac{1}{2}} \tag{25}$$

and then λ_{cr} as follows:

$$\lambda_{cr}=k^2\left(1+\beta^2\right)^2\left(\varphi-\frac{k^2\left(1+\beta^2\right)^2}{3\left(\frac{2\mathrm{D}}{E\hbar}\frac{K_P}{K_K}\left(1+\chi\frac{K_W}{K_K}\right)^{-1}\left(1+3\beta^2+3\beta^4+\beta^6\right)\right)}\right)-\frac{1}{E\hbar}\left(\frac{E\hbar\alpha_x}{1-\upsilon}\Delta T+\eta\hbar H_x^2\right)+\frac{\rho^2}{\left(1+\beta^2\right)^2}+\frac{1}{E\hbar}\left(1+\chi\frac{K_W}{K_K}\right)^{-1}\Bigg[K_W\left(\varphi-\frac{k^2\left(1+\beta^2\right)^2}{3\left(\frac{2\mathrm{D}}{E\hbar}\frac{K_P}{K_K}\left(1+\chi\frac{K_W}{K_K}\right)^{-1}\left(1+3\beta^2+3\beta^4+\beta^6\right)\right)}\right)^{-1}+K_P\left(1+\beta^2\right)+\mathrm{D}\frac{K_P}{K_K}\left(1+3\beta^2+3\beta^4+\beta^6\right)\left(\varphi-\frac{k^2\left(1+\beta^2\right)^2}{3\left(\frac{2\mathrm{D}}{E\hbar}\frac{K_P}{K_K}\left(1+\chi\frac{K_W}{K_K}\right)^{-1}\left(1+3\beta^2+3\beta^4+\beta^6\right)\right)}\right)^2\Bigg] \tag{26}$$

In the case of Winkler and Pasternak models, the Eq. (19) can be simplified as follows:

$$\lambda(p,\beta)=k^2\left(1+\beta^2\right)^2p^2-\frac{1}{E\hbar}\left(\frac{E\hbar\alpha_x}{1-\upsilon}\Delta T+\eta\hbar H_x^2\right)+\frac{\rho^2}{\left(1+\beta^2\right)^2}+\frac{1}{E\hbar}\left[\frac{K_W}{p^2}+K_P\left(1+\beta^2\right)\right] \tag{27}$$

By minimizing the buckling load $\lambda(p,\beta)$ in Eq. (27) we obtain a polynomial of degree 4, which allows us to write:

$$p_{cr} = \left(\frac{\frac{K_W}{E\hbar} + \frac{\rho^2}{\left(1+\beta^2\right)^2}}{k^2\left(1+\beta^2\right)^2} \right)^{\frac{1}{4}} \tag{28}$$

and then λ_{cr} can be written in the following simplified form:

$$\lambda_{cr} = k^2\left(1+\beta^2\right)^2 \sqrt{\frac{\frac{K_W}{E\hbar} + \frac{\rho^2}{\left(1+\beta^2\right)^2}}{k^2\left(1+\beta^2\right)^2}} - \frac{1}{E\hbar}\left(\frac{E\hbar\alpha_x}{1-\upsilon}\Delta T + \eta\hbar H_x^2\right) + \frac{\rho^2}{\left(1+\beta^2\right)^2} + \frac{1}{E\hbar}\left[K_W \sqrt{\frac{k^2\left(1+\beta^2\right)^2}{\frac{K_W}{E\hbar} + \frac{\rho^2}{\left(1+\beta^2\right)^2}}} + K_P\left(1+\beta^2\right)\right] \tag{29}$$

5. Numerical analysis

5.1 Validation of analytical formulas for buckling of embedded SWCNTs on elastic foundation under coupled effects of magnetic field and temperature change

In this section, parameters used for analysis are the following: $h = 0.066nm$, $a = 0.142nm$, $E = 5500GPa$, $\upsilon = 0.34$, $\beta = 0.6$, $e_0 = 0$, $K_W = 50nN/nm^3$, $K_G = 5nN/nm$, $K_C = 10nN/nm^3$(Timesli 2020b). We assume that $\alpha_x = 2.5 \times 10^{-5}K^{-1}$, $H_x = 0.1A/nm$, $\Delta T = 20°K$. Fig.4 presents the critical buckling load λ_{cr} of SWCNT versus radius R. The critical load decreases with increasing radius R, it increases in the presence of Winkler, Pasternak and Kerr foundations compared to that without medium. These results also show that λ_{cr} of the Pasternak model is more important than that of Winkler and Kerr. Note that there is an agreement between the numerical results obtained by minimization and those analytical.

Using the analytical formula (26), Fig. 5 presents the variations of λ_{cr} versus radius R with and without applying the effects of the magnetic field and temperature change. As shown in this figure, the local critical load increases by applying a magnetic field and decreases with a temperature change.

5.2 Effect of the nonlocal parameter on the buckling behavior

In the following numerical tests and using the same data in the section 5.1 and Eq. (18), we show the small-scale effects on the critical buckling load λ_{cr} of SWCNTs embedded in an elastic foundation. Fig. 6(a) explains that λ_{cr} decreases with increasing the nonlocal parameter e_0. It can be seen that the difference between the critical buckling loads of different values of e_0 is quite large for small values of R, which indicates that the small-scale effect can be neglected for the critical buckling load when the radius R is large.

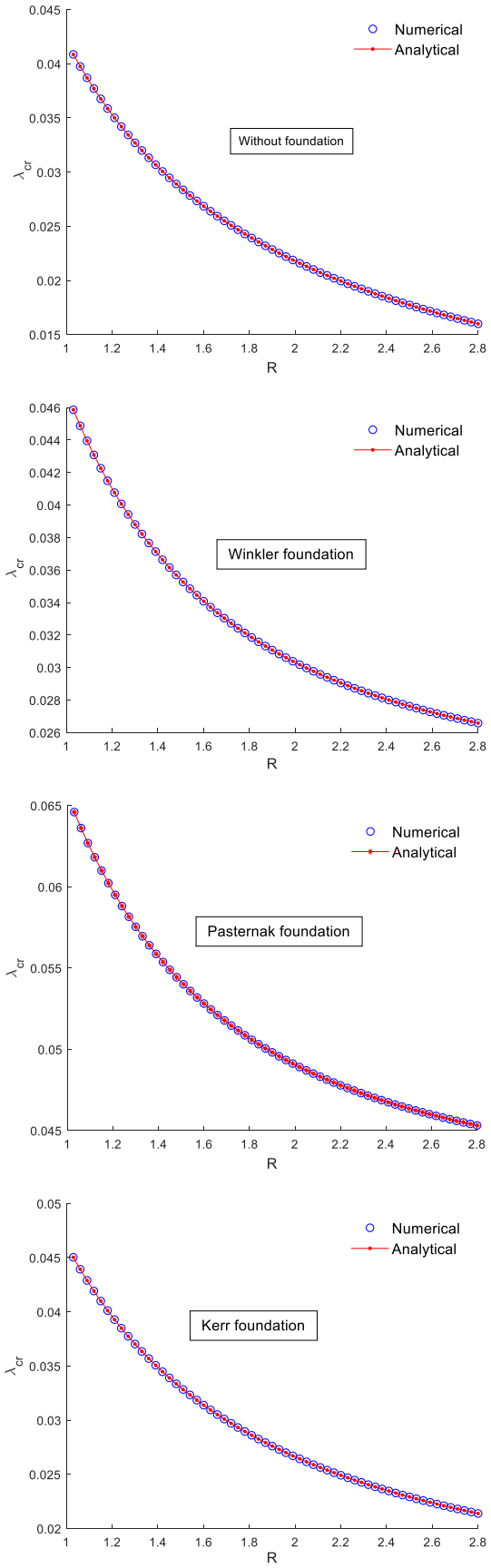

Fig. 4 Comparison between analytical and numerical results for the absence and presence of Winkler-, Pasternak-and Kerr-type elastic foundation

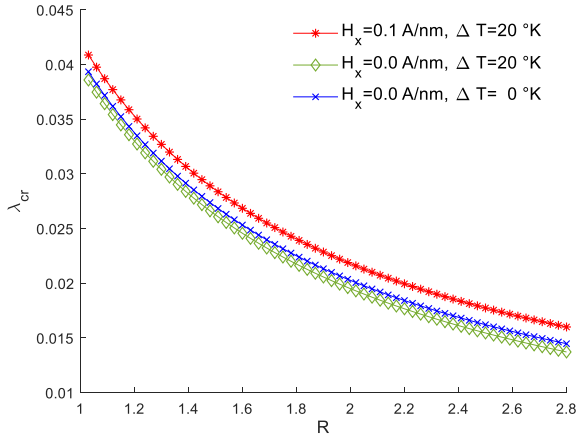

Fig. 5 Effects of magnetic field and temperature change on local buckling behavior

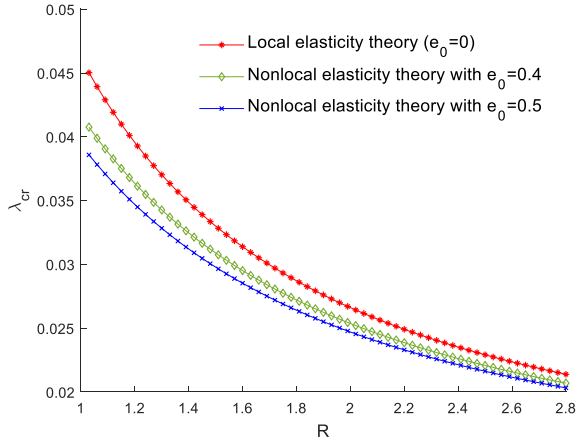

(a) λ_{cr} versus R for different values of e_0

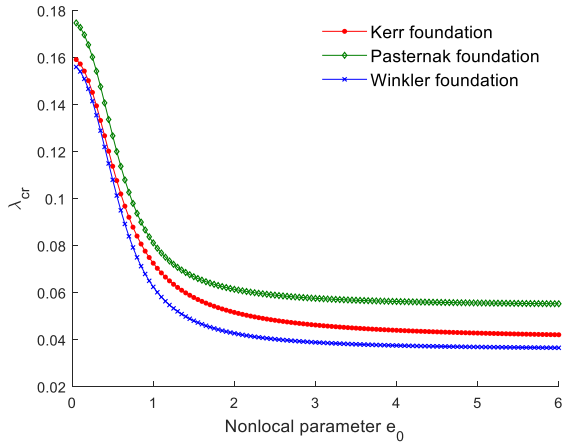

(b) λ_{cr} versus e_0 for Winkler-, Pasternak-and Kerr-type elastic foundation

Fig. 6 Effect of radius R and nonlocal parameter e_0 on the buckling behavior of CNT

The effect of the foundation type on the buckling load of CNT versus the nonlocal parameter is plotted in Fig. 6(b). This figure shows that the effect of Pasternak foundation on the buckling of CNT is more important compared to Winkler and Kerr foundations. On the other hand, λ_{cr} descend most quickly with increasing e_0, if the value of e_0 exceeds a certain value ($e_0 \simeq 2$) the decrease in λ_{cr} becomes gradually slower. This result shows that the nonlocal parameter e_0 has strong effects on the buckling behavior of CNT for small values of e_0.

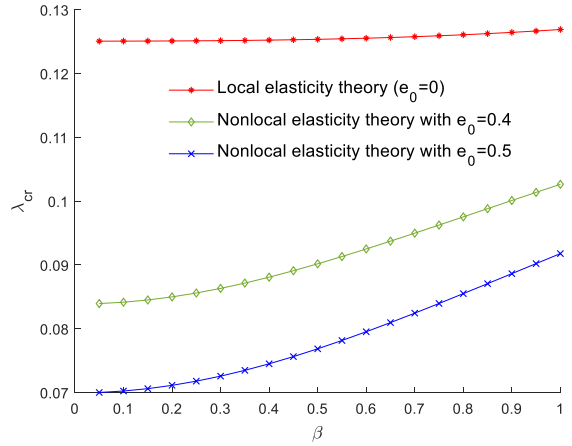

Fig. 7 The critical buckling load versus aspect ratio β for different values of the nonlocal parameter

In the following we consider that $R = 0.34$ nm. According to Fig. 7, the critical buckling load λ_{cr} of CNTs increases when the aspect ratio β increases. λ_{cr} rises most quickly with increasing β for nonlocal elasticity theory.

5.3 Effect of magnetic field strength on buckling behavior

It is displayed in Fig. 8(a) that the critical buckling load increases exponentially as the magnetic field strength increases. It is because that increasing magnetic field leads stiffer structure. We can conclude that the impact of the applied magnetic field has improved the mechanical properties of CNT.A further investigation revealed the same trend in DWCNT, TWCNT, QWCNT, etc. These results on the buckling behavior of CNTs show that the stability of CNT can be achieved using the proposed model.

The effect of the magnetic field on the buckling load of the CNT versus nonlocal parameter is plotted in Fig. 8(b). This figure explains that the effect of the magnetic field on the buckling of the CNT becomes more important at lower nonlocal parameters.

5.4 Effect of change in temperature on buckling behavior

The impact of change in temperature on buckling behavior of SWCNT is presented in Fig. 9. It is clearly seen that increase in temperature change at low temperature decreases the critical buckling load as shown in Fig. 9. Such response is due to the fact that the Young modulus and the rigidity of the CNT decrease at low temperature (or room temperature) and such causes the CNT to become increasingly less rigid as the temperature change increases. However, the increase in temperature change at high temperature increases the critical buckling load of CNT.

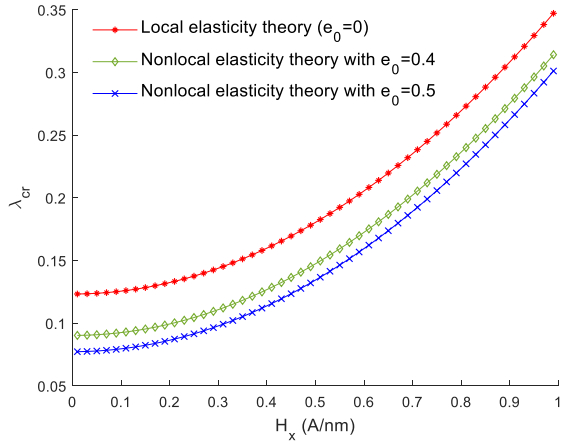

(a) λ_{cr} versus H_x for different values of e_0.

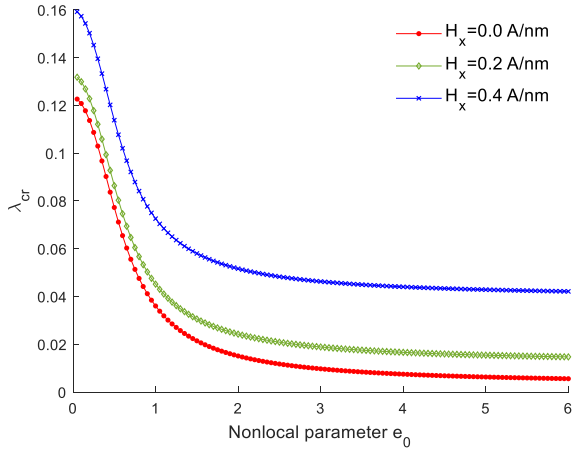

(b) λ_{cr} versus e_0 for different values of H_x.

Fig. 8 Effect of magnetic field strength on buckling behavior of CNT

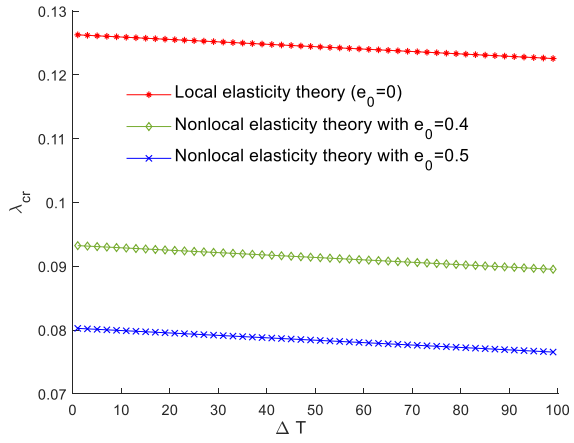

Fig. 9 Effect of change in temperature on buckling behavior

5.5 Study of the number of walls effect

Fig. 10 shows that increasing the number of layers N leads to decrease in λ_{cr}. It can be seen that the difference between the critical buckling loads of different values of e_0

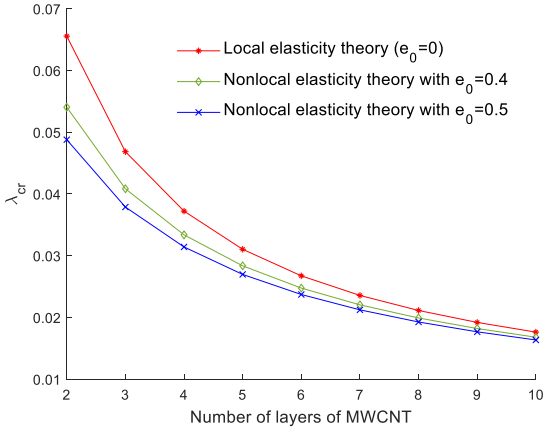

Fig. 10 The critical buckling load versus number of layers for different nonlocal parameter values

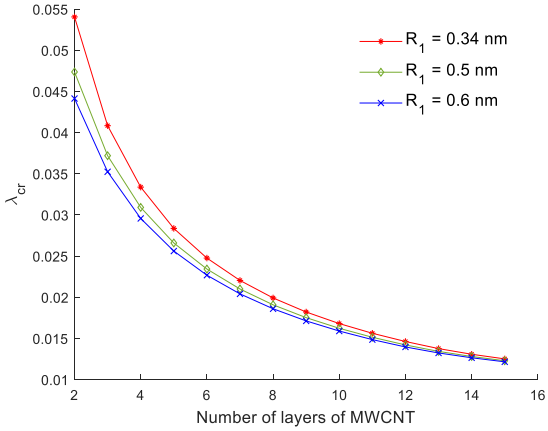

Fig. 11 The critical buckling load versus number of layers for different values of internal radius R_1 of the MWCNT

is quite large for small values of N (or small outermost radius R_N), which indicates that the small-scale effect plays an important role for the critical buckling loads when the number of layers is small (or the outermost radius R_N is small). We can also conclude that as the outermost radius increases, the difference between these results becomes very small and their values tend towards the local critical buckling loads. This implies that the effect of the nonlocal parameter is very small for MWCNT with large radii and it can be neglected.

It can also be seen in Fig. 11 that as the number of layers increases, the influence of the internal radius R_1 becomes neglected and the critical buckling loads tend towards the local critical buckling loads.

6. Conclusions

A continuum cylindrical shell model has been investigated for the buckling analysis of SWCNT and MWCNT embedded in an elastic foundation and under coupled effects of the magnetic field, temperature change, and number of walls. The interaction between the CNT and the elastic medium is treated as Winkler, Pasternak and Kerr

elastic models. Analytical formulas of the local critical buckling load are developed for SWCNT embedded in elastic medium. Otherwise, an optimization technique is used to obtain the nonlocal critical buckling load of SWCNT and MWCNT resting on elastic foundations and under coupled effects of the magnetic field, temperature change, and number of walls. Several numerical studies have been conducted to show the effects of many parameters such as the nonlocal parameter, the magnetic field, the temperature change and the number of walls. Through the parametric studies, the following results are established:

• Increase in the magnetic field strength causes the increase in the critical buckling load λ_{cr}. The significant effect of this parameter on the buckling behavior of CNTs shows that it can be used to achieve the stability or control the instability of CNTs.

• The effect of the magnetic field on the values of critical buckling loads reduces with the effect of the nonlocal parameter.

• Increase in the change in temperature leads to the decrease in λ_{cr} for the low temperature and to the increase in λ_{cr} for the high temperature. This is because the coefficient of thermal expansion of CNT is positive at high temperature and negative at low/room temperature.

• The effect of the nonlocal parameter can be neglected for MWCNT with a large number of layers.

• λ_{cr} increases with increasing aspect ratio β.

• λ_{cr} of SWCNT and MWCNT increases with increasing elastic foundation parameters.

• Under coupled effects of the magnetic field, temperature change, SWCNT and MWCNT resting on Pasternak foundation have the highest critical buckling load values. The effect of the Pasternak foundation parameter is more significant than the Winkler- and Kerr-type foundation parameter.

• The increase in the number of layers decreases the rigidity of embedded MWCNT under the simultaneous effects of magnetic field and temperature change.

These results will help in the design of CNT for various structural, electrical, mechanical and biological applications in a thermal and magnetic environment.

References

Ajiki, H. and Ando, T. (1996), "Energy Bands of Carbon Nanotubes in Magnetic Fields", *J. Phys. Soc. Japan*, **65**(2), 505-514. https://doi.org/10.1143/JPSJ.65.505.

Al-Furjan, M.S.H., Habibi, M., Ni, J., Jung, D.W., and Tounsi, A. (2020a), "Frequency simulation of viscoelastic multi-phase reinforced fully symmetric systems", *Eng. Comput.*, 1-17. https://doi.org/10.1007/s00366-020-01200-x

Al-Furjan, M.S.H., Habibi, M., Rahimi, A., Chen, G., Safarpour, H., Safarpour, M. and Tounsi, A. (2020b), "Chaotic simulation of the multi-phase reinforced thermo-elastic disk using GDQM", *Eng. Comput.*, 1-24. https://doi.org/10.1007/s00366-020-01144-2.

Al-Furjan, M.S.H., Habibi, M., Jung, D.w., Sadeghi, S., Safarpour, H., Tounsi, A. and Chen, G. (2020c), "A computational framework for propagated waves in a sandwich doubly curved nanocomposite panel", *Eng. Comput.*, 1-18. https://doi.org/10.1007/s00366-020-01130-8.

Al-Furjan, M.S.H., Safarpour, H., Habibi, M., Safarpour, M. and Tounsi, A. (2020d), "A comprehensive computational approach for nonlinear thermal instability of the electrically FG-GPLRC disk based on GDQ method", *Eng. Comput.*, 1-18. https://doi.org/10.1007/s00366-020-01088-7.

Al-Furjan, M.S.H., Hatami, A., Habibi, M., Shan, L. and Tounsi, A. (2021), "On the vibrations of the imperfect sandwich higher-order disk with a lactic core using generalize differential quadrature method", *Compos. Struct.*, **257**, 113150. https://doi.org/10.1016/j.compstruct.2020.113150.

Amara, K., Youb, O., Bouazza, M., Tounsi, A. and El Abbas, A.B. (2014), "Influence of temperature change on column Buckling of double walled carbon nanotubes using different theories", *Energy Procedia*, **50**, 634-641. https://doi.org/10.1016/j.egypro.2014.06.078.

Aminikhah, H. and Hemmatnezhad, M. (2011), "Nonlinear vibrations of multiwalled carbon nanotubes under various boundary conditions", *Int. J. Differ. Equ.*, **2011**, 343576. https://doi.org/10.1155/2011/343576.

Arshid, E., Khorasani, M., Soleimani-Javid, Z., Amir, S., and Tounsi, A., (2021), "Porosity-dependent vibration analysis of FG microplates embedded by polymeric nanocomposite patches considering hygrothermal effect via an innovative plate theory", *Eng. Comput.*, 1-22. https://doi.org/10.1007/s00366-021-01382-y.

Arda, M. and Aydogdu, M. (2018), "Longitudinal Magnetic Field Effect on Torsional Vibration of Carbon Nanotubes", *Mater. Horiz.*, **49**(2), 304-313. https://doi.org/10.22059/jcamech.2018.269982.344.

Asghar, S., Naeem, M.N., Hussain, M.,Taj, M. and Tounsi, A. (2020), "Prediction and assessment of nonlocal natural frequencies of DWCNTs: Vibration analysis", *Comput. Concrete*, **25**(2), 133-144. https://doi.org/10.12989/cac.2020.25.2.133.

Balubaid, M., Tounsi, A., Dakhel, B. and Mahmoud, S.R. (2019), "Free vibration investigation of FG nanoscale plate using nonlocal two variables integral refined plate theory", *Comput. Concrete*, **24**(6), 579-586. http://doi.org/10.12989/cac.2019.24.6.579.

Bao, W.X., Zhu, C.C. and Cui, W.Z. (2004), "Simulation of Young's modulus of single-walled carbon nanotubes by molecular dynamics", *Physica B*, **352**(1), 156-163. https://doi.org/10.1016/j.physb.2004.07.005.

Bellal, M., Hebali, H., Heireche, H., Bousahla, A.A., Tounsi, A.J., Bourada, F., Mahmoud, S.R., Bedia, E.A.A. and Tounsi, A. (2020), "Buckling behavior of a single-layered graphene sheet resting on viscoelastic medium via nonlocal four-unknown integral model", *Steel Compos. Struct.*, **34**(5), 643-655. http://doi.org/10.12989/scs.2020.34.5.643

Bellucci, S., González, J., Guinea, F., Onorato, P. and Perfetto, E. (2007), "Magnetic field effects in carbon nanotubes", *J. Condens. Matter Phys.*, **19**(39), 395017. https://doi.org/10.1143/JPSJ.65.505.

Bendenia, N., Zidour, M., Bousahla, A.A., Bourada, F., Tounsi, A., Benrahou, K.H., Adda Bedia, E.A., Mahmoud, S.R. and Tounsi, A. (2020), "Deflections, stresses and free vibration studies of FG-CNT reinforced sandwich plates resting on Pasternak elastic foundation", *Comput. Concr.*, **26**(3), 213-226. http://doi.org/10.12989/cac.2020.26.3.213.

Bensattalah, T., Bouakkaz, K., Zidour, M. and Daouadji, T.M. (2018), "Critical buckling loads of carbon nanotube embedded in Kerr's medium", *Adv. Nano Res.*, **6**(4), 339-356. https://doi.org/10.12989/anr.2018.6.4.339.

Berghouti, H., Bedia, E.A.A., Benkhedda, A. and Tounsi, A. (2019), "Vibration analysis of nonlocal porous nanobeams made of functionally graded material", *Adv. Nano Res.*, **7**(5), 351-364. http://doi.org/10.12989/anr.2019.7.5.351.

Bourada, F., Bousahla, A.A., Tounsi, A.J., Bedia, E.A.A, Mahmoud, S.R., Benrahou, K.H. and Tounsi, A. (2020), "Stability and dynamic analyses of SW-CNT reinforced concrete beam resting on elastic-foundation", *Comput. Concr.*, **25**(6), 485-495. http://doi.org/10.12989/cac.2020.25.6.485.

Bousahla, A.A., Bourada, F., Mahmoud, S.R., Tounsi, A.J., Algarni, A., Bedia, E.A.A. and Tounsi, A. (2020), "Buckling and dynamic behavior of the simply supported CNT-RC beams using an integral-first shear deformation theory", *Comput. Concr.*, **25**(2), 155-166. http://doi.org/10.12989/cac.2020.25.2.155.

Boutaleb, S., Benrahou, K.H., Bakora, A., Algarni, A., Bousahla, A.A., Tounsi, A., Tounsi, A. and Mahmoud, S.R. (2019), "Dynamic analysis of nanosize FG rectangular plates based on simple nonlocal quasi 3D HSDT", *Adv. Nano Res.*, **7**(3), 191-208. http://doi.org/10.12989/anr.2019.7.3.191.

Brush, D. and Almroth, B. (1975), *Buckling of Bars, Plates and Shells*, McGraw-Hill, New York, U.S.A.

Calvert, P. (1999), "A recipe for strength", *Nature*, **399**(6733), 210-211. https://doi.org/10.1038/20326.

Cao, Q., Fan, Q., Chen, Q., Liu, C., Han, X. and Li, L. (2020), "Recent advances in manipulation of micro- and nano-objects with magnetic fields at small scales", *Mater. Horiz.*, **7**(3), 638-666. https://doi.org/10.1039/C9MH00714H

Deng, L., Young, R.J., Kinloch, I.A., Sun, R., Zhang, G., Noé, L. and Monthioux, M. (2014), "Coefficient of thermal expansion of carbon nanotubes measured by Raman spectroscopy", *Appl. Phys. Lett.*, **104**(5), 051907. http://doi.org/10.1063/1.4864056.

Donnell, L.H. (1934), "Stability of thin-walled tubes under torsion", TR-479; N.A.C.A.

Ebrahimi, F., Hosseini, S.H.S., Singhal, A. (2020), "A comprehensive review on the modeling of smart piezoelectric nanostructures", *Struct. Eng. Mech.*, **74**(5), 611-633. http://doi.org/10.12989/sem.2020.74.5.611.

Eringen, A.C. (1972a), "Nonlocal polar elastic continua", *Int. J. Eng. Sci.*, **10**(1), 1-16. https://doi.org/10.1016/0020-7225(72)90070-5

Eringen, A.C. (1972b), "Linear theory of nonlocal elasticity and dispersion of plane waves", *Int. J. Eng. Sci.*, **10**(5), 425-435. https://doi.org/10.1016/0020-7225(72)90050-X.

Eringen, A.C. (1983), "On differential equations of nonlocal elasticity and solutions of screw dislocation and surface waves", *J. Appl. Phys.*, **54**(9), 4703-4710. https://doi.org/10.1063/1.332803.

Eringen, A.C. (2002), *Nonlocal Continuum Field Theories*, Springer, New York, U.S.A.

Eringen, A.C. and Edelen, D.G.B. (1972), "On nonlocal elasticity", *Int. J. Eng. Sci.*, **10**(3), 233-248. https://doi.org/10.1016/0020-7225(72)90039-0.

Falvo, M.R., Clary, G.J., Taylor, R.M., Chi, V. and Brooks, F.P. (1997), "Bending and buckling of carbon nanotubes under large strain", *Nature*, **389**(6651), 582-584. https://doi.org/10.1038/39282.

Fedorov, G., Tselev, A., Jimenez, D., Latil, S., Kalugin, N.G., Barbara, P., Smirnov, D. and Roche, S. (2007), "Magnetically induced field effect in carbon nanotube devices", *Nano Lett.*, **7**(4), 960-964. https://doi.org/10.1021/nl063029v.

Fu, Y.M., Hong, J.W. and Wang, X.Q. (2006), "Analysis of nonlinear vibration for embedded carbon nanotubes", *J. Sound Vib.*, **296**(4-5), 746-756. https://doi.org/10.1016/j.jsv.2006.02.024.

Gul, U. and Aydogdu, M. (2018), "Noncoaxial vibration and buckling analysis of embedded double-walled carbon nanotubes by using doublet mechanics", *Compos. Part B Eng.*, **137**, 60-73. https://doi.org/10.1016/j.compositesb.2017.11.005.

Heidari, F., Taheri, K., Sheybani, M., Janghorban, M., and Tounsi, A. (2021), "On the mechanics of nanocomposites reinforced by wavy/defected/aggregated nanotubes", *Steel Compos. Struct.*, **38**(5), 533-545. https://doi.org/10.12989/scs.2021.38.5.533

Hernandez, E., Goze, C., Bernier P. and Rubio, A. (1998), "Elastic properties of C and BxCyNz composite nanotubes", *Phys. Rev. Lett.*, **80**(20), 4502-4505. https://doi.org/10.1103/PhysRevLett.80.4502.

Hussain, M., Naeem, M.N., Taj, M. and Tounsi, A. (2020), "Simulating vibrations of vibration of single-walled carbon nanotube using Rayleigh-Ritz's method", *Adv. Nano Res.*, **8**(3), 215-228. https://doi.org/10.12989/anr.2020.8.3.215.

Hussain, M., Naeem, M.N., Tounsi, A. and Taj, M. (2019), "Nonlocal effect on the vibration of armchair and zigzag SWCNTs with bending rigidity", *Adv. Nano Res.*, **7**(6), 431-442. http://doi.org/10.12989/anr.2019.7.6.431.

Iijima, S. (1991), "Helical microtubules of graphitic carbon", *Nature*, **354**(6348), 56-58. https://doi.org/10.1038/354056a0.

Iijima, S., Brabec, C., Maiti, A. and Bernholc, J. (1996), "Structural flexibility of carbon nanotubes", *J. Chem. Phys.*, **104**(5), 2089-2092. https://doi.org/10.1063/1.470966.

Jena, S.K., Chakraverty, S. and Malikan, M. (2020), "Vibration and buckling characteristics of nonlocal beam placed in a magnetic field embedded in Winkler-Pasternak elastic foundation using a new refined beam theory: An analytical approach", *Eur. Phys. J. Plus*, **135**(2), 164. https://doi.org/10.1140/epjp/s13360-020-00176-3.

Jiang, J.W., Wang, J.S. and Li, B. (2009), "Thermal expansion in single-walled carbon nanotubes and graphene: Nonequilibrium Green's function approach", *Phys. Rev. B.*, **80**(20), 205429. http://doi.org/10.1103/PhysRevB.80.205429.

Karami, B., Janghorban, M., Shahsavari, D. and Tounsi, A. (2018), "A size-dependent quasi-3D model for wave dispersion analysis of FG nanoplates", *Steel Compos. Struct.*, **28**(1), 99-110. https://doi.org/10.12989/scs.2018.28.1.099.

Karami, B., Janghorban, M. and Tounsi, A. (2019a), "On pre-stressed functionally graded anisotropic nanoshell in magnetic field", *J Braz. Soc. Mech. Sci. Eng.*, **41**, 495. https://doi.org/10.1007/s40430-019-1996-0.

Karami, B., Janghorban, M. and Tounsi, A. (2019b), "Galerkin's approach for buckling analysis of functionally graded anisotropic nanoplates/different boundary conditions", *Eng. Comput.*, **35**(4), 1297-1316. https://doi.org/10.1007/s00366-018-0664-9

Kuzumaki, T., Miyazawa, K., Ichinose, H. and Ito, K. (1998), "Processing of carbon nanotube reinforced aluminum composites", *J. Mater. Res.*, **13**(9), 2445-2449. https://doi.org/10.1557/JMR.1998.0340.

Lee, D.W., Kim, S.H., Kozlov M.E., Lepró, X., Baughman, R.H. and Kim, S.J. (2018), "Magnetic torsional actuation of carbon nanotube yarn artificial muscle", *RSC Advances*, **8**(31), 17421-17425. https://doi.org/10.1039/C8RA01040D.

Liew, K.M., Wong, C.H., He, X.Q., Tan, M.J. and Meguid, S.A. (2004), "Nanomechanics of single and multiwalled carbon nanotubes", *Phys. Rev. B*, **69**(11), 115429. https://doi.org/10.1103/PhysRevB.69.115429

Malikan, M. (2020), "On the plastic buckling of curved carbon nanotubes", *Theor. App. Mech. Lett.*, **10**(1), 46-56. https://doi.org/10.1016/j.taml.2020.01.004.

Malikan, M. and Eremeyev, V.A. (2020), "Post-critical buckling of truncated conical carbon nanotubes considering surface effects embedding in a nonlinear Winkler substrate using the Rayleigh-Ritz method", *Mater. Res. Express*, **7**(2), 025005. https://doi.org/10.1088/2053-1591/ab691c.

Matouk, H., Bousahla, A.A., Heireche, H., Bourada, F., Bedia, E.A.A., Tounsi, A. and Benrahou, K.H. (2020), "Investigation on hygro-thermal vibration of P-FG and symmetric S-FG nanobeam using integral Timoshenko beam theory", *Adv. Nano*

Res., **8**(4), 293-305. http://doi.org/10.12989/anr.2020.8.4.293.
Mohamed, N., Mohamed, S.A. and Eltaher, M.A. (2020) "Buckling and post-buckling behaviors of higher order carbon nanotubes using energy-equivalent model", *Eng*. *Comput*., **37**(4), 2823-2836. https://doi.org/10.1007/s00366-020-00976-2.
Medani, M., Benahmed, A., Zidour, M., Heireche, H., Tounsi, A., Bousahla, A.A., Tounsi, A.J. and Mahmoud, S.R. (2019) "Static and dynamic behavior of (FG-CNT) reinforced porous sandwich plate using energy principle", *Steel Compos*. *Struct*., **32**(5), 595-610. http://doi.org/10.12989/scs.2019.32.5.595.
Ponnusamy, P. and Amuthalakshmi, A. (2015), "Influence of thermal and magnetic field on vibration of double walled carbon nanotubes using nonlocal Timoshenko beam theory", *Procedia Mater*. *Sci*., **10**, 243-253. https://doi.org/10.1016/j.mspro.2015.06.047.
Rai, R.S. and Bajpai, V. (2021), "Recent advances in ZnO nanostructures and their future perspective", *Adv*. *Nano Res*., **11**(1), 37-54. https://doi.org/10.12989/anr.2021.11.1.037.
Rahmani, R. and Antonov, M. (2019), "Axial and torsional buckling analysis of single- and multi-walled carbon nanotubes: finite element comparison between armchair and zigzag types", *SN Appl*. *Sci*., **1**(9), 1134. https://doi.org/10.1007/s42452-019-1190-0.
Ru, C.Q. (2000), "Column buckling of multiwall carbon nanotubes with interlayer radial displacement", *Phys*. *Rev*. *B*., **62**(24), 16962-16967. https://doi.org/10.1103/PhysRevB.62.16962.
Rouabhia, A., Chikh, A., Bousahla, A.A., Bourada, F., Heireche, H., Tounsi, A.J., Benrahou, K.H., Tounsi, A. and Al-Zahrani, M.M. (2020), "Physical stability response of a SLGS resting on viscoelastic medium using nonlocal integral first-order theory", *Steel Compos*. *Struct*., **37**(6), 695-709. http://doi.org/10.12989/scs.2020.37.6.695.
Sanchez-Portal, D., Artacho, E., Soler, J. M., Rubio, A., Ordejón, P. (1999), "Ab-initio structural, elastic, and vibrational properties of carbon nanotubes", *Phys*. *Rev*. *B*, **59**(19), 12678-12688. https://doi.org/10.1103/PhysRevB.59.12678.
Schadler, L.S., Giannaris, S.C. and Ajayan, P.M. (2018), "Load transfer in carbon nanotubes epoxy composites", *Appl*. *Phys*. *Lett*., **73**(26), 3842-3844. https://doi.org/10.1063/1.122911.
Shahsavari, D., Karami, B. and Mansouri, S. (2018), "Shear buckling of single layer graphene sheets in hygrothermal environment resting on elastic foundation based on different nonlocal strain gradient theories", *Eur*. *J*. *Mech*. *A Solids*, **67**, 200-214. https://doi.org/10.1016/j.euromechsol.2017.09.004.
Sobamowo, M.G., Akanmu, J.O., Adeleye, O.A., Akingbade, S.A. and Yinusa, A.A. (2021), "Coupled effects of magnetic field, number of walls, geometric imperfection, temperature change, and boundary conditions on nonlocal nonlinear vibration of carbon nanotubes resting on elastic foundations", *Force*. *Mech*., **3**, 100010. https://doi.org/10.1016/j.finmec.2021.100010.
Soleimani-Javid, Z., Arshid, E., Khorasani, M., Amir, S. and Tounsi, A. (2021), "Size-dependent flexoelectricity-based vibration characteristics of honeycomb sandwich plates with various boundary conditions", *Adv*. *Nano Res*., **10**(5), 449-460. https://doi.org/10.12989/anr.2021.10.5.449.
Taj, M., Majeed, A., Hussain, M., Naeem, M.N., Safeer, M., Ahmad, M., Khan, H.U. and Tounsi, A. (2020), "Non-local orthotropic elastic shell model for vibration analysis of protein microtubules", *Comput*. *Concr*., **25**(3), 245-253. https://doi.org/10.12989/cac.2020.25.3.245
Timesli, A. (2020a), "Prediction of the critical buckling load of SWCNT reinforced concrete cylindrical shell embedded in an elastic foundation", *Comput*. *Concrete*, **26**(1), 53-62. https://doi.org/10.12989/cac.2020.26.1.053
Timesli, A. (2020b), "Buckling analysis of double walled carbon nanotubes embedded in Kerr elastic medium under axial compression using the nonlocal Donnell shell theory", *Adv*. *Nano Res*., **9**(2), 69-82. https://doi.org/10.12989/anr.2020.9.2.069.
Timesli, A. (2020c), "An efficient approach for prediction of the nonlocal critical buckling load of double-walled carbon nanotubes using the nonlocal Donnell shell theory", *SN Appl*. *Sci*., **2**(3), 247. https://doi.org/10.1007/s42452-020-2182-9.
Timesli, A. (2021), "Analytical modeling of buckling behavior of porous FGM cylindrical shell embedded within an elastic foundation", *Gazi Univ*. *J*. *Sci*., **1**(1). https://doi.org/10.35378/gujs.860783.
Timesli, A., Braikat, B., Jamal, M. and Damil, N. (2017), "Prediction of the critical buckling load of multi-walled carbon nanotubes under axial compression", *Comptes Rendus Mécanique*, **345**(2), 158-168. https://doi.org/10.1007/s42452-020-2182-9.
Van Vinh, P., Tounsi, A. (2021), "The role of spatial variation of the nonlocal parameter on the free vibration of functionally graded sandwich nanoplates", *Eng*. *Comput*., 1-19. https://doi.org/10.1007/s00366-021-01475-8.
Wang, H., Zandi, Y., Gholizadeh, M., and Issakhov, A. (2021), "Buckling of porosity-dependent bi-directional FG nanotube using numerical method", *Adv*. *Nano Res*., **10**(5), 493-507. http://doi.org/10.12989/anr.2021.10.5.493.
Wu, C.P., Chen, Y.H., Hong, Z.L. and Lin, C.H. (2018), "Nonlinear vibration analysis of an embedded multi-walled carbon nanotube", *Adv*. *Nano Res*., **6**(2), 163-182. https://doi.org/10.12989/anr.2018.6.2.163.
Xie, B., Li, Q., Zeng, K, Sahmani, S. and Madyira, D.M. (2020), "Instability analysis of silicon cylindrical nanoshells under axial compressive load using molecular dynamics simulations", *Microsyst*. *Technol*., **26**(12), 3753-3764. https://doi.org/10.1007/s00542-020-04851-4.
Yacobson, B.I., Brabec, C.J. and Bernhole, J. (1996), "Nanomechanics of carbon nanotubes: instabilities beyound linear response", *Phys*. *Rev*. *Lett*., **76**(14), 2511-2514. https://doi.org/10.1103/PhysRevLett.76.2511.
Yan, X., Itoh, T., Kitahama, Y., Suzuki, T., Sato, H., Miyake, T. and Ozaki, Y. (2012), "A Raman spectroscopy study on single-wall carbon nanotube/polystyrene nanocomposites: Mechanical compression transferred from the polymer to single-wall carbon nanotubes", *J*. *Phys*. *Chem*. *C*, **116**(33), 17897-17903. https://doi.org/10.1021/jp303509g.
Yazid, M., Heireche, H., Tounsi, A., Bousahla, A.A. and Houari, M.S.A. (2018), "A novel nonlocal refined plate theory for stability response of orthotropic single-layer graphene sheet resting on elastic medium", *Smart Struct*. *Syst*., **21**(1), 15-25. https://doi.org/10.12989/sss.2018.21.1.015.
Zerrouki, R., Karas, A., Zidour, M., Bousahla, A.A., Tounsi, A., Bourada, F., Tounsi, A.J., Benrahou, K.H. and Mahmoud, S.R. (2021), "Effect of nonlinear FG-CNT distribution on mechanical properties of functionally graded nano-composite beam", *Struct*. *Eng*. *Mech*., **78**(2), 117-124. http://doi.org/10.12989/sem.2021.78.2.117.
Zhou, L., Cheny, F. and Zhao, Z. (2019), "Subharmonic bifurcation and chaos of a carbon nanotube supported by a Winkler and Pasternak foundation", *Int*. *J*. *Mod*. *Phys*. *B*, **33**(19), 1950207. https://doi.org/10.1142/S0217979219502072.

AT

Nomenclature

x	Axial coordinate
θ	Circumferential angular coordinate
Δ^2	Bi-laplacian operator
E	Equivalent Young Modulus of Elasticity for CNT
ν	Poisson's ratio
h	Equivalent shell thickness of CNT
D	Bending stiffness of the shell
S	Cross sectional area of the nanotube
w	Transverse displacement of the reference surface
c	Transverse displacement of the reference surface
a	Carbon-carbon bonds length
$\mu = e_0 a$	Scaling parameter for the small-scale effects
R	Radius of the nanotube
R_i	Radius of the i^{th} tube of nanotube layers
L	Length of the nanotube
N_{xx}	Normal forces according to x
$N_{\theta\theta}$	Normal forces according to θ
$N_{x\theta}$	Internal shear force
T	Change in temperature
H_x	Magnetic field strength
α_x	Coefficient of thermal expansion
η	Magnetic field permeability
$ES\alpha_x T$	Constant axial force due to thermal effects
$\eta S H_x^2$	Magnetic force per unit length due to Lorentz force
U	External axial pressure
$\lambda = U/(Eh)$	Load parameter of the external axial pressure
F_i	VdW force between the i^{th} tube and the $(i\text{-}1)^{\text{th}}$ tube
c_i	Coefficient of the VdW force between the i^{th} tube and the $(i\text{-}1)^{\text{th}}$ tube
f	Pressure of elastic foundations
K_W	Lower spring constant / Winkler foundation constant
K_P	Intermediate shear constant / Pasternak foundation constant
K_K	Upper spring constant / Kerr foundation constant
ϕ	Stress function
n	Circumferential half wavenumbers
m	Axial half wavenumbers
E_i^m	Elliptic integrals
ξ	Depth of Lennard-Jones potential
σ	Parameter being determined by the equilibrium distance